

Sahel rainfall projections constrained by past sensitivity to global warming

Jacob Schewe¹ and Anders Levermann¹

¹Potsdam Institute for Climate Impact Research

November 24, 2022

Abstract

Africa's central Sahel region has experienced prolonged drought conditions in the past, while rainfall has recovered more recently. Global climate models project anything from no change to a strong wetting trend under unabated climate change; and they have difficulty reproducing the complex historical record. Here we show that when a period of dominant aerosol forcing is excluded, a consistent wetting response to greenhouse-gas induced warming emerges in observed rainfall. Using the observed response coefficient estimate as a constraint, we find that CMIP6 climate models with a realistic past rainfall response show a smaller spread, and higher median, of projected future rainfall change, compared to the full ensemble. In particular, very small or negative rainfall trends are absent from the constrained ensemble. Our results provide further evidence for a robust Sahel rainfall increase in response to greenhouse-gas forcing, consistent with recent observations, and including the possibility of a very strong increase.

1 **Sahel rainfall projections constrained by past**
2 **sensitivity to global warming**

3 **Jacob Schewe¹, Anders Levermann^{1,2,3}**

4 ¹Potsdam Institute for Climate Impact Research, 14473 Potsdam, Germany

5 ²Institute of Physics, Potsdam University, Potsdam, Germany

6 ³Columbia University, New York, USA

7 **Key Points:**

- 8 • We identify the response of Sahel rainfall to greenhouse gas-induced global warm-
9 ing in the historical record
- 10 • Many global climate models of the latest generation (CMIP6) do not reproduce
11 the observed rainfall response
- 12 • Observational constraint reduces model spread and implies stronger rainfall in-
13 crease under further warming than in full ensemble

Corresponding author: Jacob Schewe, schewe@pik-potsdam.de

Abstract

Africa's central Sahel region has experienced prolonged drought conditions in the past, while rainfall has recovered more recently. Global climate models project anything from no change to a strong wetting trend under unabated climate change; and they have difficulty reproducing the complex historical record. Here we show that when a period of dominant aerosol forcing is excluded, a consistent wetting response to greenhouse-gas induced warming emerges in observed rainfall. Using the observed response coefficient estimate as a constraint, we find that CMIP6 climate models with a realistic past rainfall response show a smaller spread, and higher median, of projected future rainfall change, compared to the full ensemble. In particular, very small or negative rainfall trends are absent from the constrained ensemble. Our results provide further evidence for a robust Sahel rainfall increase in response to greenhouse-gas forcing, consistent with recent observations, and including the possibility of a very strong increase.

Plain Language Summary

Rainfall is a critical resource for a large population in the African Sahel region, but rainfall levels have strongly varied in the past. It is unclear what will happen in the next decades, because some climate models suggest little to no change in average rainfall, while other models project a strong increase due to climate change. Our study aims to narrow down this uncertainty. In the past, both greenhouse gases and aerosols influenced Sahel rainfall, to different degrees during different periods; and models may not capture both mechanisms equally well. However, future rainfall changes will likely be driven mainly by greenhouse gas levels. We identify models that closely match the rainfall change that was observed in a recent period with dominant greenhouse gas forcing. These models also tend to project stronger rainfall increases than other models. Indeed, their multi-model mean projection is an increase by almost 50% by 2040; while none of them projects stable rainfall levels or even a reduction. Thus, it appears more likely now that rainfall in the Sahel will increase substantially over the next few decades.

1 Introduction

The Sahel region is home to a large and growing population (Guengant, 2017), to whom rainfall represents a critical resource for agriculture and other economic activities, but also a source of natural hazards such as flooding (Tschakert et al., 2010). On multidecadal timescales, the first half of the 20th century has seen a rising trend in average Sahel rainfall, though frequently punctuated by anomalously dry years. This trend reversed in the second half of the century, and culminated in a prolonged period of drought conditions throughout the 1970s and 1980s that led to widespread famine and ecological deterioration. Since the 1990s, average rainfall has been rising again.

The importance and the variable history of Sahel rainfall prompt questions about its future evolution, which require an understanding of its drivers. Theoretical and modeling studies have shown that the long-term trends observed in the 20th century were to a large extent a forced response to anthropogenic changes – greenhouse-gas and aerosol (precursor) emissions –, rather than an expression of internal variability of the climate system (Giannini et al., 2008). However, future projections from global climate models show considerable disagreement over the magnitude, and partly even the sign, of the expected response to future forcing scenarios (Giannini et al., 2008; Schewe & Levermann, 2017; Monerie et al., 2020). In this paper, we apply recent understanding of the causes of 20th century rainfall trends in order to narrow the range of future rainfall projections in the latest generation of global climate models.

61 A series of studies have shown that differences in sea surface temperature (SST)
62 between the (sub-tropical) North Atlantic, and the tropical Atlantic or global oceans,
63 can explain a large part of the observed Sahel rainfall variations on interannual and longer
64 timescales (Biasutti et al., 2008; Giannini et al., 2013). These SST differences, in turn,
65 are modulated by human-induced radiative forcings. Greenhouse-gas (GHG) emissions,
66 which have been rising at a growing rate throughout the 20th century, increase surface
67 temperatures globally and persistently. On the other hand, scattering aerosols, mainly
68 sulfate aerosols related to sulfur dioxide (SO₂) emissions from the use fossil fuels, have
69 a cooling effect on SST, which however is more localized and transient due to the shorter
70 lifetime of tropospheric aerosols, compared to GHG.

71 The multi-decadal variations in Sahel rainfall have recently been attributed to the
72 specific combination of these two forcings during the 20th century (Giannini & Kaplan,
73 2019). Specifically, the GHG-induced warming, in the tropics, increases atmospheric sta-
74 bility because surface warming is quickly disseminated vertically through deep convec-
75 tion, and then horizontally within the tropical upper atmosphere. This raises the ener-
76 getic threshold for convection (Chou & Neelin, 2004). Rainfall at the margins of convec-
77 tive regions then depends on whether sufficient moisture gets imported at the lower level
78 to meet this “upped ante”. It has been argued that the massive SO₂ emissions in the
79 decades after World War II, in Europe and North America, and the resultant regional
80 cooling effect of sulfate aerosols on North Atlantic SST, acted to limit moisture supply
81 from the subtropical North Atlantic to the African monsoon (Giannini & Kaplan, 2019).
82 When moisture import became increasingly insufficient to meet the rising convective thresh-
83 old, this led to the observed decline in Sahel rainfall starting in the 1950s and acceler-
84 ating in the 1960s. After aerosol precursor emissions in the North Atlantic sector declined
85 in the 1980s and 1990s, subtropical North Atlantic SSTs rose in correspondance with the
86 global GHG forcing, low-level atmospheric moisture content was able to catch up with
87 the “upped ante”, and Sahel rainfall began to increase again.

88 This understanding implies that the response of Sahel rainfall to global warming
89 is markedly different depending on whether or not GHG-induced warming is opposed
90 by regional aerosol-induced cooling in the North Atlantic. Given that aerosol and aerosol
91 precursor emissions in the North Atlantic sector are projected to remain low through-
92 out the 21st century (Rao et al., 2017), it is the response to GHG-induced warming alone
93 that will likely dominate the future evolution of Sahel rainfall. Thus, climate models which
94 simulate that response accurately may also be suited for future projections, no matter
95 whether or not they also capture the response to combined GHG and aerosol forcing well.

96 2 Data

97 We investigate the historical and SSP5-8.5 experiments from 39 models participat-
98 ing in the Coupled Model Intercomparison Project phase 6 (CMIP6) (Eyring et al., 2016;
99 O’Neill et al., 2016; Tebaldi et al., 2021). Where multiple realizations are available for
100 a given model and experiment, we use only the first one. We focus on July–September
101 average rainfall in the central Sahel region (0–30°E, 10–20°N), which is more suscepti-
102 ble to changes in remote moisture import than the coastal regions further to the West.
103 Notably, the western Sahel is also more susceptible to slow changes in ocean circulation
104 following atmospheric warming, and therefore shows a different long-term response to
105 GHG emissions than the central Sahel (Monerie et al., 2021). To account for the pos-
106 sibility that models may get the monsoon dynamics qualitatively right but not the pre-
107 cise spatial distribution of rainfall anomalies, we also perform our analysis on rainfall av-
108 eraged over model-specific, rectangular regions chosen to include the largest simulated
109 rainfall anomaly, which are often somewhat offset from the common region denoted above.
110 The corresponding figures, as well as a list of models analyzed, are provided in Support-
111 ing Information.

112 Observational temperature and precipitation data are obtained from the Univer-
113 sity of East Anglia Climatic Research Unit (CRU) TS4.04 dataset (Harris et al., 2020).
114 Anthropogenic SO₂ emission data are obtained from the Community Emissions Data Sys-
115 tem (CEDS) (Hoesly et al., 2018); these data are also used as input for the CMIP6 his-
116 torical experiments.

117 3 Results

118 Under the high GHG concentration scenario SSP5-8.5, most of the CMIP6 mod-
119 els project an increase in central Sahel rainfall in the course of the 21st century (Fig. 1
120 and Supporting Information Fig. S1). By the 2040s, the multi-model mean is about 25%
121 above recent levels (Fig. 1(a), grey line); and comparing the end of the 21st century to
122 the 20th century average, the multi-model mean increase is around 70% (Supporting In-
123 formation Fig. S1). However, the spread across the model ensemble is large. Individual
124 models project near-zero or even small negative changes in rainfall, while at the other
125 extreme, some models show increases of around 200%, i.e., a tripling of average rainfall
126 amounts, between the 20th century and the end of the 21st century (Fig. 1(b)). The largest
127 relative increases are found in the CanESM and EC-Earth3 models, each of which have
128 several variants in the ensemble, but which between each other are largely independent
129 (Brunner et al., 2020), highlighting that models with very large rainfall increases can-
130 not be treated as mere outliers.

131 Thus, the models in CMIP6 largely agree on the sign of the expected central Sa-
132 hel rainfall change, and more so than in previous simulation rounds (Biasutti, 2013; Park
133 et al., 2015); but given the broad and homogeneous distribution of projected rainfall changes
134 across the CMIP6 ensemble, there remains a large uncertainty about the magnitude of
135 this change. Constraining these centennial-scale projections with past observations is com-
136 plicated by the earlier finding that mean biases in past Sahel rainfall simulations are a
137 poor predictor of simulated future rainfall change (Monerie et al., 2017); and by the fact
138 that the centennial-scale trend in the observations is very small. Indeed, average rain-
139 fall amounts in the early 21st century are roughly the same as during the early 20th cen-
140 tury (Fig. 2(a)).

141 This is despite substantial decadal-scale trends in the data. In the first half of the
142 20th century, central Sahel rainfall saw a rising trend, concurrent with the trend in global
143 mean surface temperature. Beginning in the 1950s, however, rainfall gradually declined,
144 leading into a period of devastating droughts in the 1970s and 1980s. Unlike with global
145 mean temperature, which saw a relatively short period of moderate decline, the declin-
146 ing trend in Sahel rainfall did not reverse until about the late 1980s. It coincided with
147 a period of steeply rising sulfate aerosol precursor emissions in Europe and North Amer-
148 ica, as well as globally, stemming from fossil fuel combustion (shading in Fig. 2(a)).

149 Motivated by previous findings regarding Sahel rainfall response to GHG and aerosol
150 forcing (Giannini & Kaplan, 2019), we divide the historical rainfall record into three parts:
151 A period with steeply rising and, subsequently, high anthropogenic SO₂ emissions in the
152 North Atlantic sector (AER, 1951-1995); as well as the periods before (PRE, 1901-1950)
153 and after (POST, 1996-2019) this period. The PRE and POST periods correspond to
154 rising trends in Sahel rainfall and a dominant role of GHG-induced surface warming as
155 the forcing responsible for that trend; whereas the AER period corresponds to (mostly)
156 declining Sahel rainfall and an important role of sulfate aerosols in inhibiting Atlantic
157 moisture supply to the Sahel, as discussed above. We find, in both the PRE and POST
158 periods, a very similar sensitivity of Sahel rainfall to global surface warming: About 0.7
159 mm/day per degree of warming (Fig. 2(b)). This similarity suggests a coherent response
160 of Sahel rainfall to surface warming in the absence of strong aerosol forcing.

161 Given that aerosol precursor emissions, at least in the OECD countries that are
162 most relevant for North Atlantic aerosol pollution, are assumed to remain low (Rao et
163 al., 2017), future Sahel rainfall changes should be dominated by GHG forcing as long as
164 GHG concentrations keep increasing; which is the case in most SSP scenarios until the
165 2040s, and in SSP5-85 throughout the 21st century. Therefore, we use the response co-
166 efficient estimated from the POST period observations to constrain the model projec-
167 tions. We find that only ten of the 39 models fall within the 66% range of the estimated
168 coefficient of 0.72; two more models fall just outside of it (Fig. 3). About half of the mod-
169 els have a negative coefficient, i.e. they show a decrease of Sahel rainfall with global warm-
170 ing during the POST period. Using the PRE period instead, we find similar results, al-
171 though the models that fall within the 66% range of the observational estimate are not
172 exactly the same (see Supporting Information, Fig. S2). We base our discussion in the
173 main paper on the results from the POST period, since models might be more reason-
174 ably expected to reproduce this later period well given the stronger forcing and arguably
175 better observational data compared to the PRE period.

176 The models' sensitivity of Sahel rainfall to warming in the recent past is correlated
177 with the projected response to future warming, although the spread is large in particu-
178 lar among the models with a negative historical sensitivity (Fig. 3). Especially at high
179 warming, those models encompass the full spread of the ensemble, including models such
180 as AWI-CM-1-1-MR, MIROC6, and MPI-ESM1-2-LR that show both a strongly neg-
181 ative response of rainfall to past warming, and a strong future rainfall increase. In con-
182 trast, the spread is smaller across those models that fall within the 66% range of the ob-
183 served sensitivity during POST (histograms in Fig. 3). In particular, none of these mod-
184 els projects less than a 0.5 mm/day increase of average rainfall under SSP5-8.5. Most
185 project an increase of 0.6 to 1.2 mm/day at 2°C global warming, and of 1 to 2 mm/day
186 at 3.5°C warming; while one of the models with the strongest agreement with observed
187 sensitivity, NESM3, projects an increase of 3 mm/day at 3.5°C warming. Correspond-
188 ingly, the median rainfall change of the constrained ensemble is substantially higher than
189 that of the full ensemble: About 0.85 compared to 0.65 mm/day at 2°C, and 1.4 com-
190 pared to 1.0 mm/day at 3.5°C.

191 In terms of relative changes within the next two decades, the multi-model mean
192 of the constrained ensemble projects a rainfall increase by nearly 50% by the 2040s, com-
193 pared to about 25% in the full ensemble (Fig. 1, blue line). This difference grows to al-
194 most 100% (constrained ensemble) versus about 50% (full ensemble) by the end of the
195 century; all relative to recent rainfall levels (Supporting Information Fig. 1). Analysis
196 of monthly rainfall changes shows that while some CMIP6 models project a substantial
197 drying in the beginning of the rainy season, this is not observed in the constrained en-
198 semble: All models whose sensitivity to historical warming is close to the observed one,
199 also show an increase of rainfall throughout the rainy season in the future (Fig. 4). This
200 is consistent with the idea of an intensifying West African monsoon system in a warm-
201 ing atmosphere with increasing moisture supply from oceanic evaporation.

202 The spatial distribution of rainfall anomalies and the location of the strongest rain-
203 fall increase in the Sahel region are not exactly the same in all models (Supporting In-
204 formation, Fig. S3), reflecting uncertainties in the dynamic response of the atmospheric
205 circulation to global warming (Monerie et al., 2020). We allow for the possibility that
206 models may simulate the response to GHG-induced forcing correctly but with some de-
207 viation in terms of the spatial pattern of rainfall and rainfall changes. To this end, we
208 select for every model a rectangular region encompassing, where present, the area of max-
209 imum rainfall increase in or near the central Sahel under SSP5-8.5. In most cases, this
210 is either identical to the common central Sahel region used so far, or offset from that re-
211 gion by a few degrees to the South and/or East (Supporting Information, Fig. S3, boxes;
212 note that boxes are chosen congruent with the respective model grid). Constraining rain-
213 fall change in these model-specific regions using the same observational estimate as be-

fore, we obtain a stronger correlation between models' historical sensitivity and projected future change (Supporting Information, Fig. S4). As before, the constraint excludes models with negative and (with one exception at 2°C warming) small positive rainfall changes, while retaining many of the models with the largest projected rainfall increases. The multi-model median projection in the constrained ensemble is again higher than in the full ensemble, though the difference is somewhat smaller than when using a common central Sahel region.

4 Conclusions

We have presented a new method to constrain central Sahel rainfall projections in global climate models, which utilizes previous findings on the relative effects of GHG and aerosol forcing and their combination. By excluding from historical data the period with strongly increasing scattering aerosol forcing in the North Atlantic sector, we quantify the rainfall response to past GHG-induced warming only, and find very similar response coefficients for two separate periods. These estimates place a strong constraint on the CMIP6 climate model simulations, in that only a minority of models exhibit a historical rainfall response that is consistent with these observations.

We note that the correlation among the model ensemble between past and projected future rainfall response to GHG-induced warming is relatively weak, especially at higher warming. This can be ascribed to a small number of models that simulate substantial drying during past periods of dominant GHG forcing, while simulating substantial wetting in the future scenario; a discrepancy that may warrant further investigation. Nevertheless, our approach does not depend on a correlation because we are constraining a mechanism (rainfall response to GHG-induced warming in the absence of strong aerosol forcing) by itself; the physical connection between the constraint and the variable of interest is therefore inherent.

The constraint consistently removes models with negative or small positive projected rainfall changes from the model ensemble, while retaining some of the models with very large rainfall increases. The multi-model median rainfall change by the end of the 21st century is substantially higher in the constrained ensemble than in the full ensemble. The same is true already by the 2040s, for which the constrained multi-model mean projects nearly a 50% increase over recent rainfall levels – a large rise over a short period during which additional GHG-induced global warming is virtually unavoidable, so that this finding holds irrespective of the SSP scenario. The constraint also removes models that project a drying in the early parts of the rainy season, retaining only models with increasing monthly mean rainfall throughout the season. These findings may aid the interpretation of climate model projections, and support the expectation that in a future dominated by GHG-induced warming, the central Sahel faces a much wetter rainy season.

Acknowledgments

The work was supported within the European Union Horizon 2020 framework (CASCADES project). The data used in this study are publicly available through the Earth System Grid Foundation (ESGF; e.g., <https://esgf-data.dkrz.de/projects/esgf-dkrz/>) for CMIP6, and at <https://catalogue.ceda.ac.uk/uuid/89e1e34ec3554dc98594a5732622bce9> for CRU. We gratefully acknowledge the CMIP6 modelling teams and the CRU for making their data available. We thank M. Büchner for help with data transfers.

References

Biasutti, M. (2013, feb). Forced Sahel rainfall trends in the CMIP5 archive. *Journal of Geophysical Research: Atmospheres*, 118(4), 1613–1623. Retrieved from

- 262 <http://onlinelibrary.wiley.com/doi/10.1002/jgrd.50206/full>
 263 doi.wiley.com/10.1002/jgrd.50206 doi: 10.1002/jgrd.50206
- 264 Biasutti, M., Held, I. M., Sobel, a. H., & Giannini, A. (2008, jul). SST Forcings
 265 and Sahel Rainfall Variability in Simulations of the Twentieth and Twenty-
 266 First Centuries. *Journal of Climate*, 21(14), 3471–3486. Retrieved from
 267 <http://journals.ametsoc.org/doi/abs/10.1175/2007JCLI1896.1> doi:
 268 10.1175/2007JCLI1896.1
- 269 Brunner, L., Pendergrass, A. G., Lehner, F., Merrifield, A. L., Lorenz, R., & Knutti,
 270 R. (2020, nov). Reduced global warming from CMIP6 projections when
 271 weighting models by performance and independence. *Earth System Dynamics*,
 272 11(4), 995–1012. Retrieved from [https://esd.copernicus.org/articles/](https://esd.copernicus.org/articles/11/995/2020/)
 273 [11/995/2020/](https://esd.copernicus.org/articles/11/995/2020/) doi: 10.5194/esd-11-995-2020
- 274 Chou, C., & Neelin, J. D. (2004, jul). Mechanisms of Global Warming Im-
 275 pacts on Regional Tropical Precipitation. *Journal of Climate*, 17(13),
 276 2688–2701. Retrieved from [http://journals.ametsoc.org/doi/abs/](http://journals.ametsoc.org/doi/abs/10.1175/1520-0442(2004)017%3C2688:MOGWIO%3E2.0.CO;2)
 277 [10.1175/1520-0442\(2004\)017%3C2688:MOGWIO%3E2.0.CO;2](http://journals.ametsoc.org/doi/abs/10.1175/1520-0442(2004)017%3C2688:MOGWIO%3E2.0.CO;2)
 278 [journals.ametsoc.org/doi/abs/10.1175/1520-0442%282004%29017%](http://journals.ametsoc.org/doi/abs/10.1175/1520-0442%282004%29017%3C2688%3AMOGWIO%3E2.0.CO;2)
 279 [3C2688%3AMOGWIO%3E2.0.CO;2](http://journals.ametsoc.org/doi/abs/10.1175/1520-0442(2004)017%3C2688:MOGWIO%3E2.0.CO;2)
 280 [http://journals.ametsoc.org/doi/](http://journals.ametsoc.org/doi/abs/10.1175/1520-0442(2004)017%3C2688:MOGWIO%3E2.0.CO;2)
 281 [10.1175/1520-0442\(2004\)017\(2688:MOGWIO\)2.0.CO;2](http://journals.ametsoc.org/doi/abs/10.1175/1520-0442(2004)017(2688:MOGWIO)2.0.CO;2) doi: 10.1175/
 1520-0442(2004)017(2688:MOGWIO)2.0.CO;2
- 282 Eyring, V., Bony, S., Meehl, G. A., Senior, C. A., Stevens, B., Stouffer, R. J., &
 283 Taylor, K. E. (2016). Overview of the Coupled Model Intercomparison Project
 284 Phase 6 (CMIP6) experimental design and organization. *Geoscientific Model*
 285 *Development*, 9(5), 1937–1958. Retrieved from [https://gmd.copernicus](https://gmd.copernicus.org/articles/9/1937/2016/)
 286 [.org/articles/9/1937/2016/](https://gmd.copernicus.org/articles/9/1937/2016/) doi: 10.5194/gmd-9-1937-2016
- 287 Giannini, A., Biasutti, M., Held, I. M., & Sobel, A. H. (2008, oct). A global per-
 288 spective on African climate. *Climatic Change*, 90(4), 359–383. Retrieved
 289 from <http://link.springer.com/10.1007/s10584-008-9396-y> doi:
 290 10.1007/s10584-008-9396-y
- 291 Giannini, A., & Kaplan, A. (2019, mar). The role of aerosols and greenhouse gases
 292 in Sahel drought and recovery. *Climatic Change*, 152(3-4), 449–466. Re-
 293 trieved from <http://link.springer.com/10.1007/s10584-018-2341-9> doi:
 294 10.1007/s10584-018-2341-9
- 295 Giannini, A., Salack, S., Lodoun, T., Ali, A., Gaye, A. T., & Ndiaye, O. (2013, jun).
 296 A unifying view of climate change in the Sahel linking intra-seasonal, interan-
 297 nual and longer time scales. *Environmental Research Letters*, 8(2), 024010. Re-
 298 trieved from <http://iopscience.iop.org/1748-9326/8/2/024010/article/>
 299 [doi: 10.1088/1748-9326/8/2/024010](http://iopscience.iop.org/1748-9326/8/2/024010/article/)
- 300 Guengant, J.-P. (2017). Africa’s Population: History, Current Status, and Projec-
 301 tions. In H. Groth & J. F. May (Eds.), *Africa’s population: In search of a de-*
 302 *mographic dividend* (pp. 11–31). Cham: Springer International Publishing. Re-
 303 trieved from https://doi.org/10.1007/978-3-319-46889-1_2 doi: 10.1007/
 304 978-3-319-46889-1_2
- 305 Harris, I., Osborn, T. J., Jones, P., & Lister, D. (2020, dec). Version 4 of the CRU
 306 TS monthly high-resolution gridded multivariate climate dataset. *Scien-*
 307 *tific Data*, 7(1), 109. Retrieved from [http://www.nature.com/articles/](http://www.nature.com/articles/s41597-020-0453-3)
 308 [s41597-020-0453-3](http://www.nature.com/articles/s41597-020-0453-3) doi: 10.1038/s41597-020-0453-3
- 309 Hawkins, E., Ortega, P., Suckling, E., Schurer, A., Hegerl, G., Jones, P., ... van
 310 Oldenborgh, G. J. (2017, sep). Estimating Changes in Global Temperature
 311 since the Preindustrial Period. *Bulletin of the American Meteorological Soci-*
 312 *ety*, 98(9), 1841–1856. Retrieved from [http://journals.ametsoc.org/doi/](http://journals.ametsoc.org/doi/10.1175/BAMS-D-16-0007.1)
 313 [10.1175/BAMS-D-16-0007.1](http://journals.ametsoc.org/doi/10.1175/BAMS-D-16-0007.1) doi: 10.1175/BAMS-D-16-0007.1
- 314 Hoesly, R. M., Smith, S. J., Feng, L., Klimont, Z., Janssens-Maenhout, G., Pitka-
 315 nen, T., ... Zhang, Q. (2018, jan). Historical (1750–2014) anthropogenic
 316 emissions of reactive gases and aerosols from the Community Emissions Data

- 317 System (CEDS). *Geoscientific Model Development*, 11(1), 369–408. Re-
318 trieved from <https://gmd.copernicus.org/articles/11/369/2018/> doi:
319 10.5194/gmd-11-369-2018
- 320 Monerie, P.-A., Pohl, B., & Gaetani, M. (2021, dec). The fast response of Sahel
321 precipitation to climate change allows effective mitigation action. *npj Climate*
322 *and Atmospheric Science*, 4(1), 24. Retrieved from [http://www.nature.com/](http://www.nature.com/articles/s41612-021-00179-6)
323 [articles/s41612-021-00179-6](http://www.nature.com/articles/s41612-021-00179-6) doi: 10.1038/s41612-021-00179-6
- 324 Monerie, P.-A., Sanchez-Gomez, E., & Boé, J. (2017, apr). On the range of future
325 Sahel precipitation projections and the selection of a sub-sample of CMIP5
326 models for impact studies. *Climate Dynamics*, 48(7-8), 2751–2770. Re-
327 trieved from <http://link.springer.com/10.1007/s00382-016-3236-y> doi:
328 10.1007/s00382-016-3236-y
- 329 Monerie, P.-A., Wainwright, C. M., Sidibe, M., & Akinsanola, A. A. (2020, sep).
330 Model uncertainties in climate change impacts on Sahel precipitation in
331 ensembles of CMIP5 and CMIP6 simulations. *Climate Dynamics*, 55(5-
332 6), 1385–1401. Retrieved from [https://link.springer.com/10.1007/](https://link.springer.com/10.1007/s00382-020-05332-0)
333 [s00382-020-05332-0](https://link.springer.com/10.1007/s00382-020-05332-0) doi: 10.1007/s00382-020-05332-0
- 334 O’Neill, B. C., Tebaldi, C., van Vuuren, D. P., Eyring, V., Friedlingstein, P., Hurtt,
335 G., . . . Sanderson, B. M. (2016, sep). The Scenario Model Intercomparison
336 Project (ScenarioMIP) for CMIP6. *Geoscientific Model Development*, 9(9),
337 3461–3482. Retrieved from [https://www.geosci-model-dev.net/9/3461/](https://www.geosci-model-dev.net/9/3461/2016/)
338 [2016/](https://www.geosci-model-dev.net/9/3461/2016/) doi: 10.5194/gmd-9-3461-2016
- 339 Park, J.-Y., Bader, J., & Matei, D. (2015, may). Northern-hemispheric differ-
340 ential warming is the key to understanding the discrepancies in the pro-
341 jected Sahel rainfall. *Nature Communications*, 6(1), 5985. Retrieved from
342 <http://www.nature.com/articles/ncomms6985> doi: 10.1038/ncomms6985
- 343 Rao, S., Klimont, Z., Smith, S. J., Van Dingenen, R., Dentener, F., Bouwman, L.,
344 . . . Tavoni, M. (2017). Future air pollution in the Shared Socio-economic Path-
345 ways. *Global Environmental Change*, 42, 346–358. Retrieved from [https://](https://www.sciencedirect.com/science/article/pii/S0959378016300723)
346 www.sciencedirect.com/science/article/pii/S0959378016300723 doi:
347 <https://doi.org/10.1016/j.gloenvcha.2016.05.012>
- 348 Schewe, J., & Levermann, A. (2017, jul). Non-linear intensification of Sahel rain-
349 fall as a possible dynamic response to future warming. *Earth System Dynam-*
350 *ics*, 8(3), 495–505. Retrieved from [https://www.earth-syst-dynam.net/8/](https://www.earth-syst-dynam.net/8/495/2017/)
351 [495/2017/](https://www.earth-syst-dynam.net/8/495/2017/) doi: 10.5194/esd-8-495-2017
- 352 Tebaldi, C., Debeire, K., Eyring, V., Fischer, E., Fyfe, J., Friedlingstein, P., . . .
353 Ziehn, T. (2021). Climate model projections from the Scenario Model Inter-
354 comparison Project (ScenarioMIP) of CMIP6. *Earth System Dynamics*, 12(1),
355 253–293. Retrieved from [https://esd.copernicus.org/articles/12/253/](https://esd.copernicus.org/articles/12/253/2021/)
356 [2021/](https://esd.copernicus.org/articles/12/253/2021/) doi: 10.5194/esd-12-253-2021
- 357 Tschakert, P., Sagoe, R., Ofori-Darko, G., & Codjoe, S. N. (2010, may). Floods in
358 the Sahel: an analysis of anomalies, memory, and anticipatory learning. *Cli-*
359 *matic Change*, 103(3-4), 471–502. Retrieved from [http://link.springer](http://link.springer.com/10.1007/s10584-009-9776-y)
360 [.com/10.1007/s10584-009-9776-y](http://link.springer.com/10.1007/s10584-009-9776-y) doi: 10.1007/s10584-009-9776-y

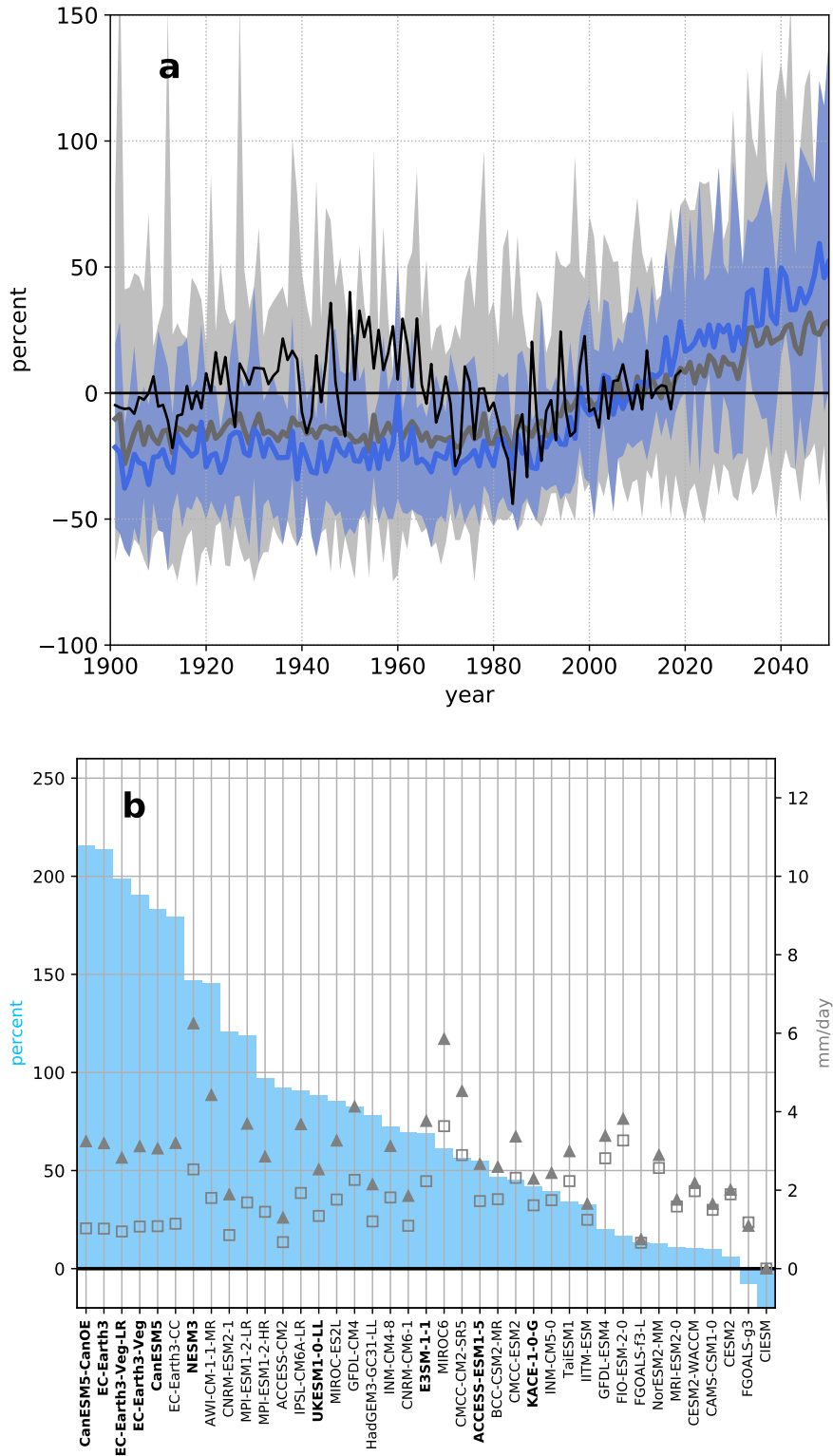


Figure 1. Sahel summer rainfall in CMIP6 coupled climate models under historical and SSP5-8.5 forcing. (a) Percentage deviation from 1996–2019 average rainfall in the full ensemble (grey) and the constrained ensemble (blue), and in observations (CRU TS v4.04, (Harris et al., 2020); thin black line). Thick lines and shading show multi-model mean and envelope (minimum and maximum among models), respectively. (b) Percentage change in simulated average rainfall by the end of the 21st century (2071–2095) compared to the 20th century average (1901–1999; bars, left vertical axis). Open squares and filled triangles show the simulated average rainfall during 1901–1999 and 2071–2095, respectively, in absolute terms (right vertical axis). The constrained ensemble is denoted by model names in bold font. An extended version of panel (a) until 2100 is provided in Supporting Information, Fig. S1.

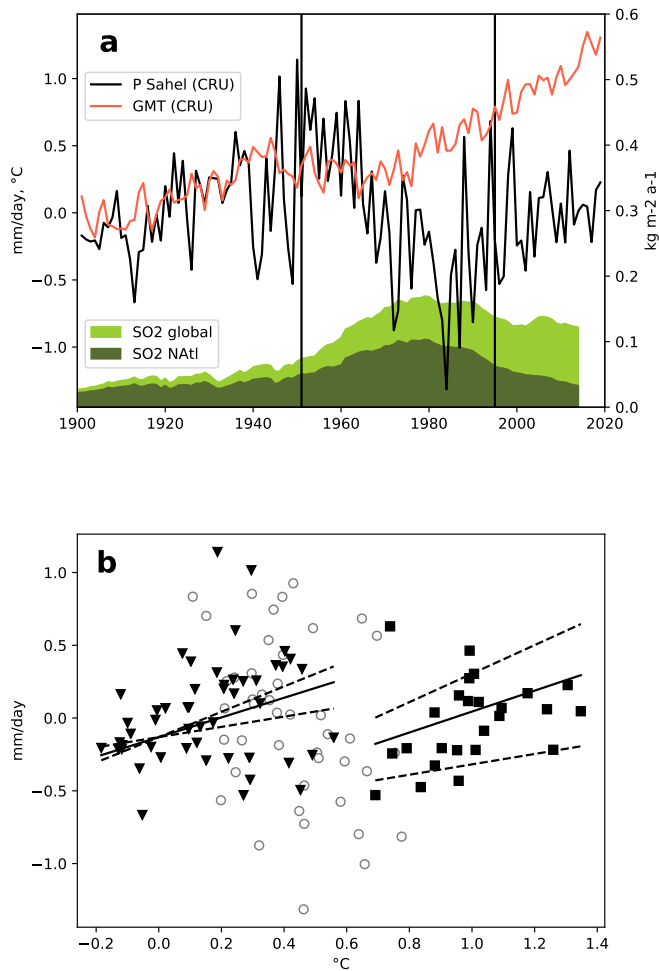


Figure 2. (a) Observed anomalies in global annual mean temperature (GMT, red) and Sahel summer rainfall (averaged over 0–30°E, 10–20°N and July–September; black), from CRU TS v4.04 (Harris et al., 2020). GMT anomalies are measured against the 1986–2005 average, and displayed relative to pre-industrial (1765–1850) conditions using an estimated warming of 0.75°C from pre-industrial up to 1986–2005 (Hawkins et al., 2017). Precipitation anomalies are relative to the 20th century average (1901–1999). Dark and light green shading shows total anthropogenic sulfur dioxide (SO₂) emissions in the North Atlantic sector (100°W–50°E, 0–90°N) and globally, respectively (Hoesly et al., 2018). (b) Sahel rainfall and GMT anomalies from (a), plotted against each other. The data is divided into a period with high SO₂ emissions in the North Atlantic sector (1951–1995, grey circles), as well as before (PRE; triangles) and after (POST; squares) this period; as indicated by the vertical lines in (a). Solid lines show Theil-Sen slopes fitted separately to the PRE and POST data, and dashed lines indicate the 66% compatibility intervals of the slope estimates. The central estimate of the slope – the sensitivity of Sahel precipitation to global warming – is 0.68 for PRE and 0.72 for POST.

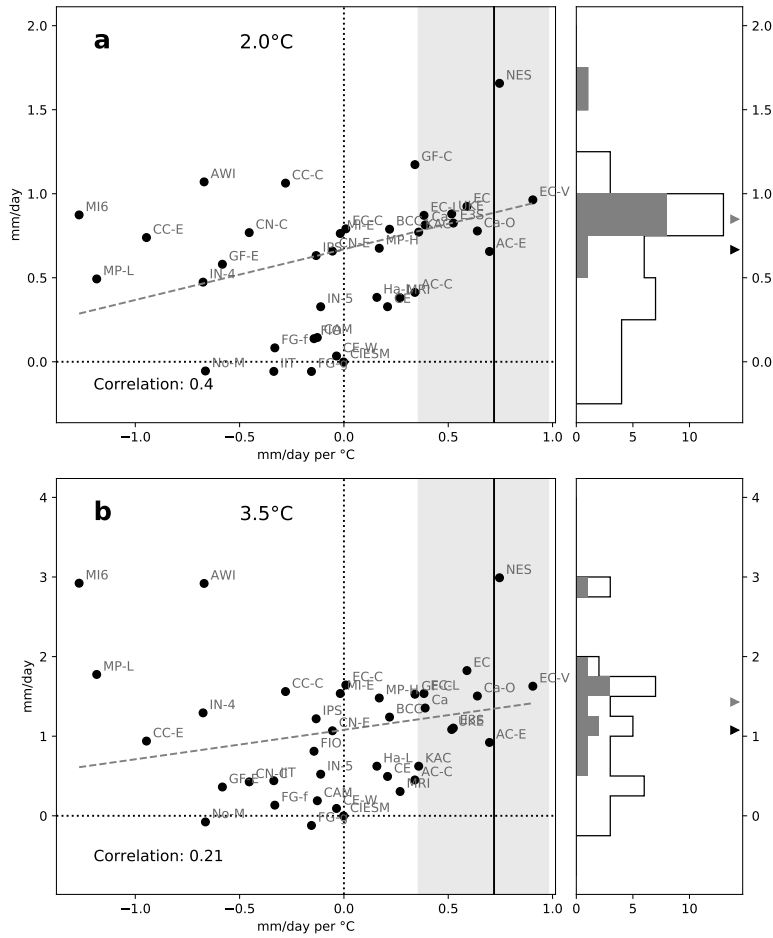


Figure 3. CMIP6 Sahel (0–30°E, 10–20°N) rainfall projections at (a) 2.0°C and (b) 3.5°C global warming, constrained with past sensitivity to GHG-induced warming. Left panels show simulated change in Sahel rainfall versus simulated historical precipitation sensitivity. Each symbol represents a CMIP6 model (see Supporting Information Table S1). Solid vertical line is the precipitation sensitivity calculated from observations (slopes in Fig. 2(b)), for the POST period. Shaded area indicates the corresponding 66% compatibility interval. Precipitation sensitivity was calculated analogously for the models. Dashed grey lines show Theil-Sen slopes. Precipitation at 0°C, 2.0°C, and 3.5°C global warming is calculated as the median of all values within a bin of 0.5°C width centered around the respective warming level, and the difference between the two levels is shown on the y-axis. Right panels show histograms of rainfall change in the full ensemble (black outline) and the ensemble of models whose precipitation sensitivity falls within the observed range (grey bars). The corresponding ensemble median is given by the black and grey triangle, respectively.

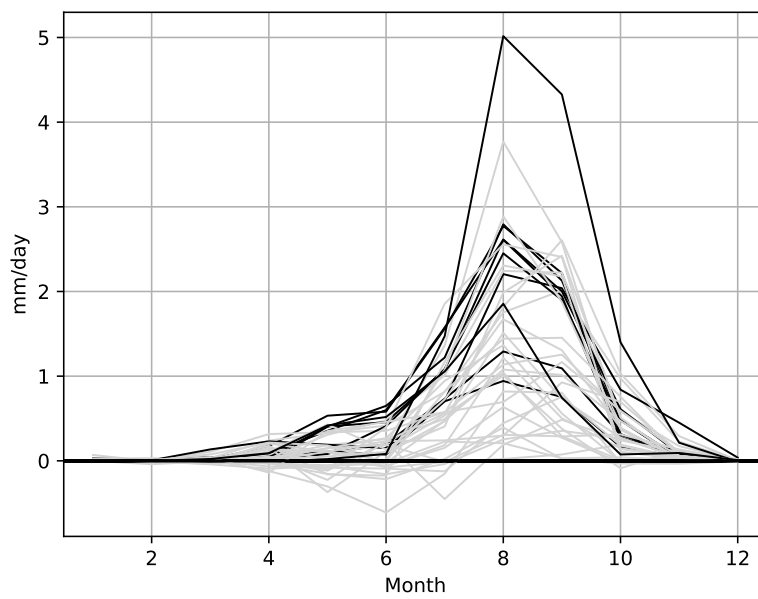


Figure 4. Change (future minus past) in monthly average Sahel ($0\text{--}30^\circ\text{E}$, $10\text{--}20^\circ\text{N}$) daily precipitation between the end of the 20th century (1970–1999) and the end of the 21st century (2070–2099). Models with historical precipitation sensitivity within the 66% range of observations (cf. Fig. 3) are shown in black, others in grey.

1 **Supporting Information for: Sahel rainfall projections**
2 **constrained by past sensitivity to global warming**

3 **Jacob Schewe¹, Anders Levermann^{1,2,3}**

4 ¹Potsdam Institute for Climate Impact Research, 14473 Potsdam, Germany

5 ²Institute of Physics, Potsdam University, Potsdam, Germany

6 ³Columbia University, New York, USA

Corresponding author: Jacob Schewe, schewe@pik-potsdam.de

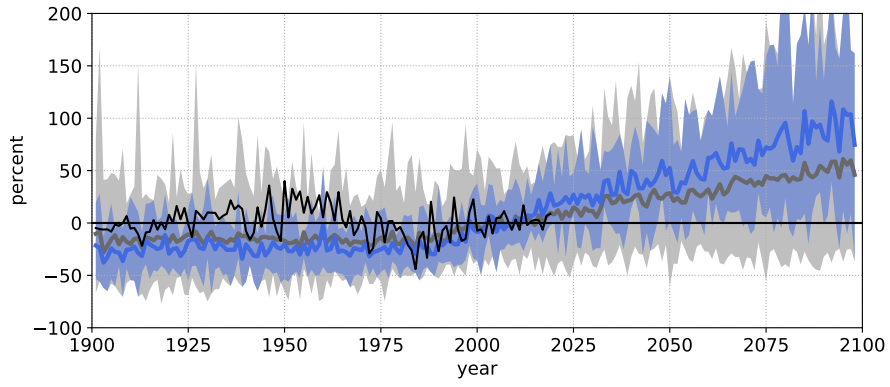


Figure S1. As Fig. 1(a) in the main paper but extending until 2100.

Table S1. CMIP6 models analyzed, with acronyms used in this study.

Acronym	Name	Institution(s) ^a
AC-C	ACCESS-CM2	CSIRO-ARCCSS
AC-E	ACCESS-ESM1-5	CSIRO
AWI	AWI-CM-1-1-MR	AWI
BCC	BCC-CSM2-MR	BCC
CAM	CAMS-CSM1-0	CAMS
Ca	CanESM5	CCCma
Ca-O	CanESM5-CanOE	CCCma
CE	CESM2	NCAR
CE-W	CESM2-WACCM	NCAR
CIESM	CIESM	THU
CC-C	CMCC-CM2-SR5	CMCC
CC-E	CMCC-ESM2	CMCC
CN-E	CNRM-CM6-1	CNRM-CERFACS
CN-C	CNRM-ESM2-1	CNRM-CERFACS
E3S	E3SM-1-1	E3SM-Project RUBISCO
EC	EC-Earth3	EC-Earth-Consortium
EC-C	EC-Earth3-CC	EC-Earth-Consortium
EC-V	EC-Earth3-Veg	EC-Earth-Consortium
EC-L	EC-Earth3-Veg-LR	EC-Earth-Consortium
FG-f	FGOALS-f3-L	CAS
FG-g	FGOALS-g3	CAS
FIO	FIO-ESM-2-0	FIO-QLNM
GF-C	GFDL-CM4	NOAA-GFDL
GF-E	GFDL-ESM4	NOAA-GFDL
Ha-L	HadGEM3-GC31-LL	MOHC NERC
IIT	IITM-ESM	CCCR-IITM
IN-4	INM-CM4-8	INM
IN-5	INM-CM5-0	INM
IPS	IPSL-CM6A-LR	IPSL
KAC	KACE-1-0-G	NIMS-KMA
MI6	MIROC-ES2L	MIROC
MI-E	MIROC6	MIROC
MP-H	MPI-ESM1-2-HR	MPI-M DWD DKRZ
MP-L	MPI-ESM1-2-LR	MPI-M AWI DKRZ DWD
MRI	MRI-ESM2-0	MRI
NES	NESM3	NUIST
No-M	NorESM2-MM	NCC
Tai	TaiESM1	AS-RCEC
UKE	UKESM1-0-LL	MOHC NERC NIMS-KMA NIWA

^aDetails at <https://wcrp-cmip.github.io/CMIP6.CV/docs/CMIP6.institution.id.html>.

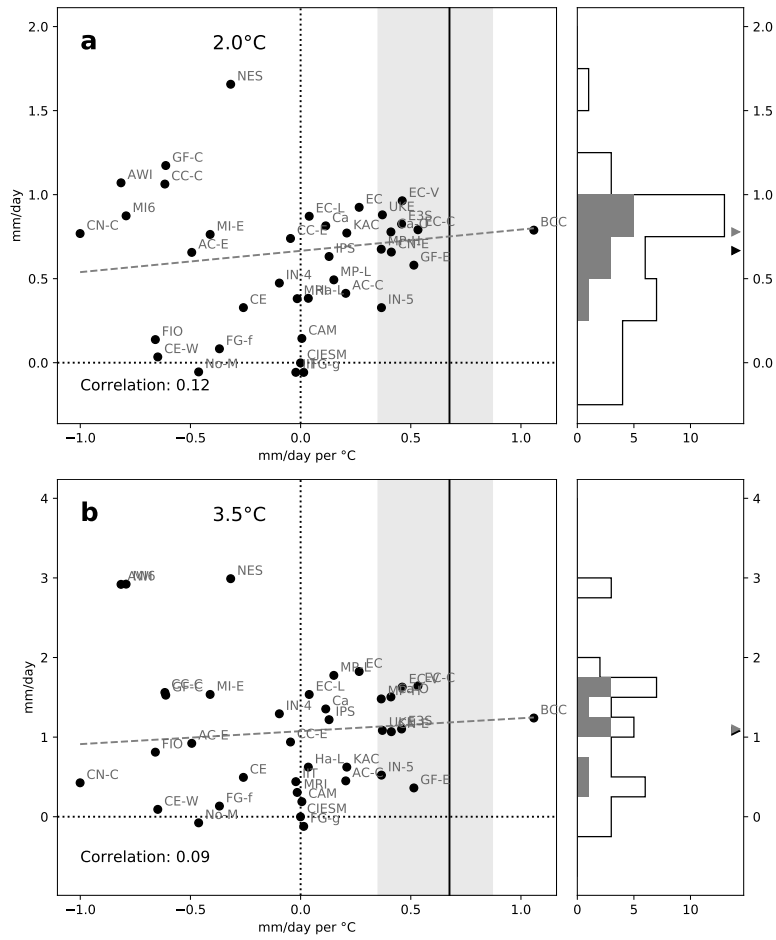


Figure S2. As Fig. 3 in the main paper but for rainfall sensitivity during the PRE period.

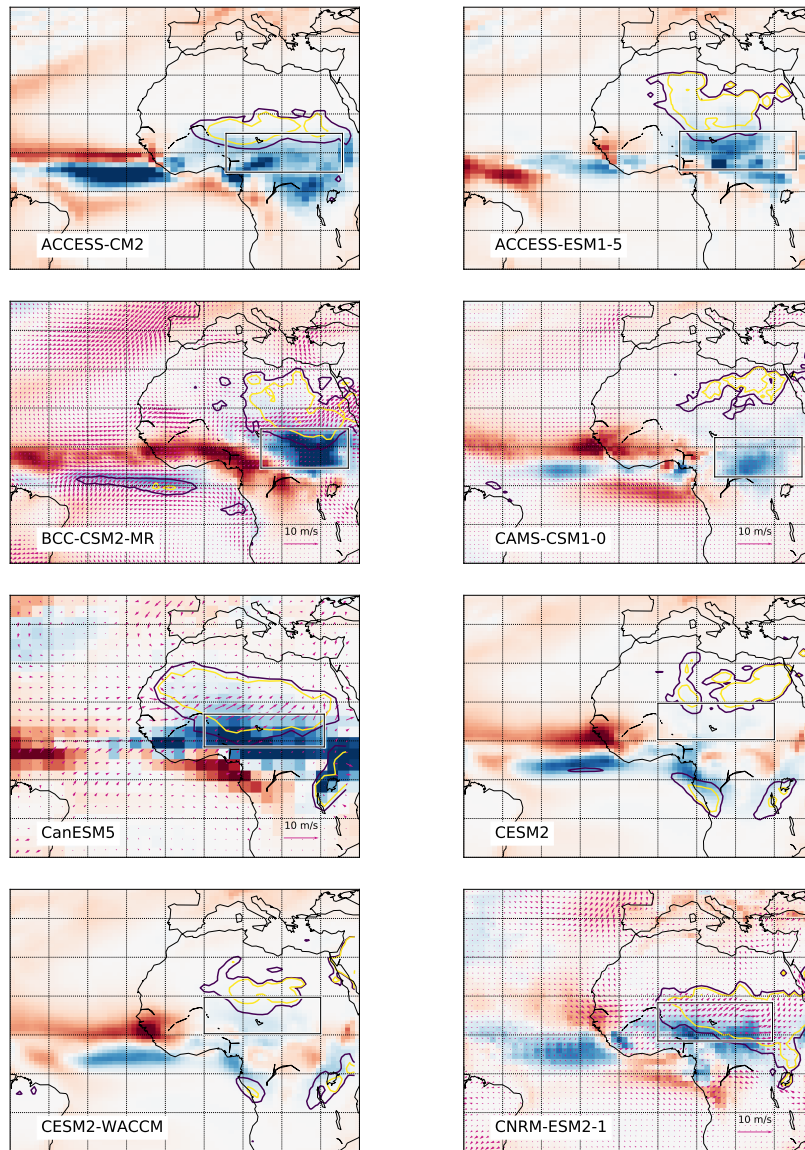


Figure S3. Simulated changes in Sahel summer climate under SSP5-8.5 in CMIP6 models. For each model the differences in July–September rainfall (colours) and near-surface wind speed (arrows) are shown between the 20th century (1900–1999) and the end of the 21st century (2070–2099). Contours indicate a doubling (blue) or tripling (yellow) of rainfall at the end of the 21st century, relative to the 20th century. Rectangles delineate model-specific regions of analysis used in subsequent Figures.

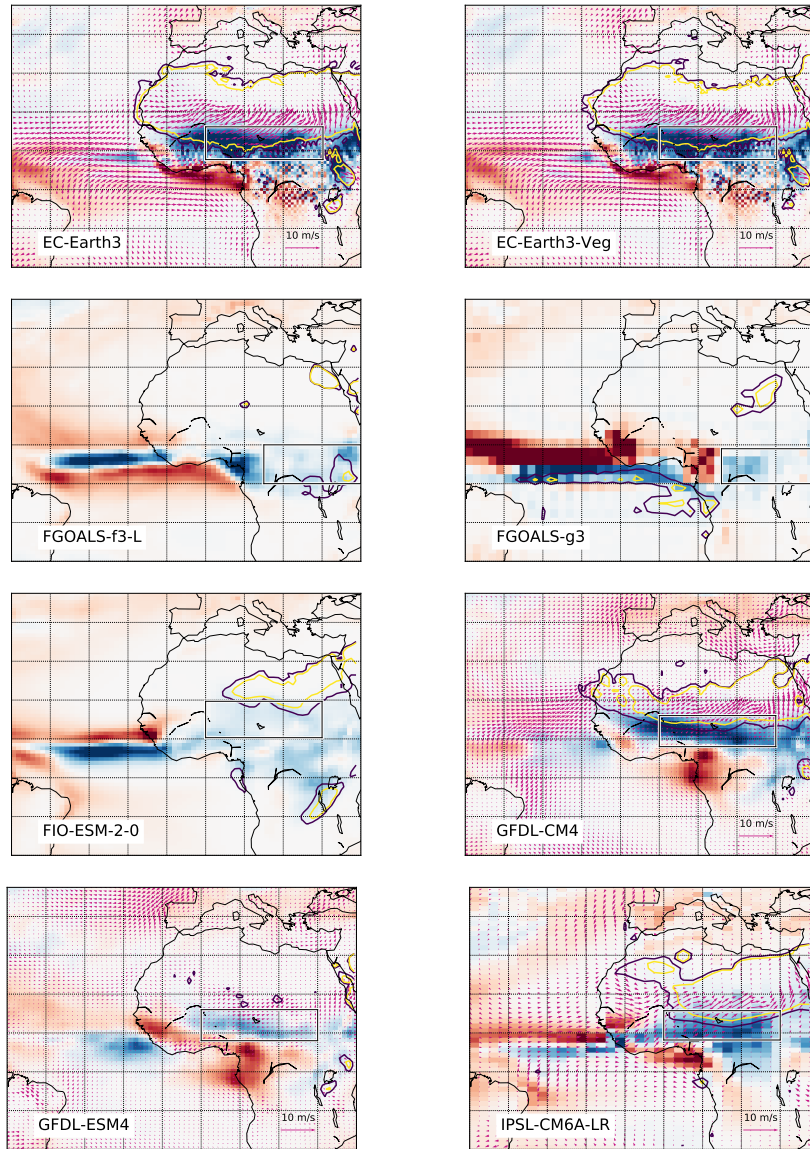


Figure S3. continued.

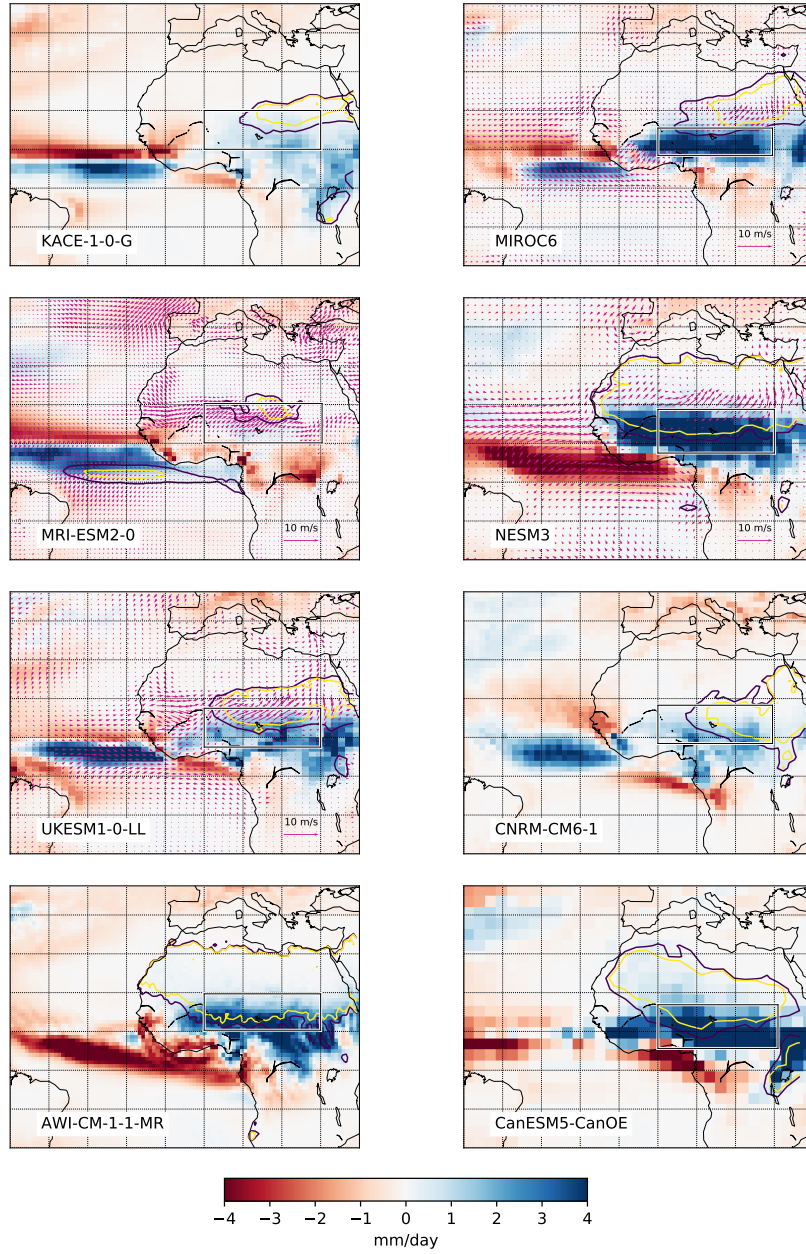


Figure S3. continued.

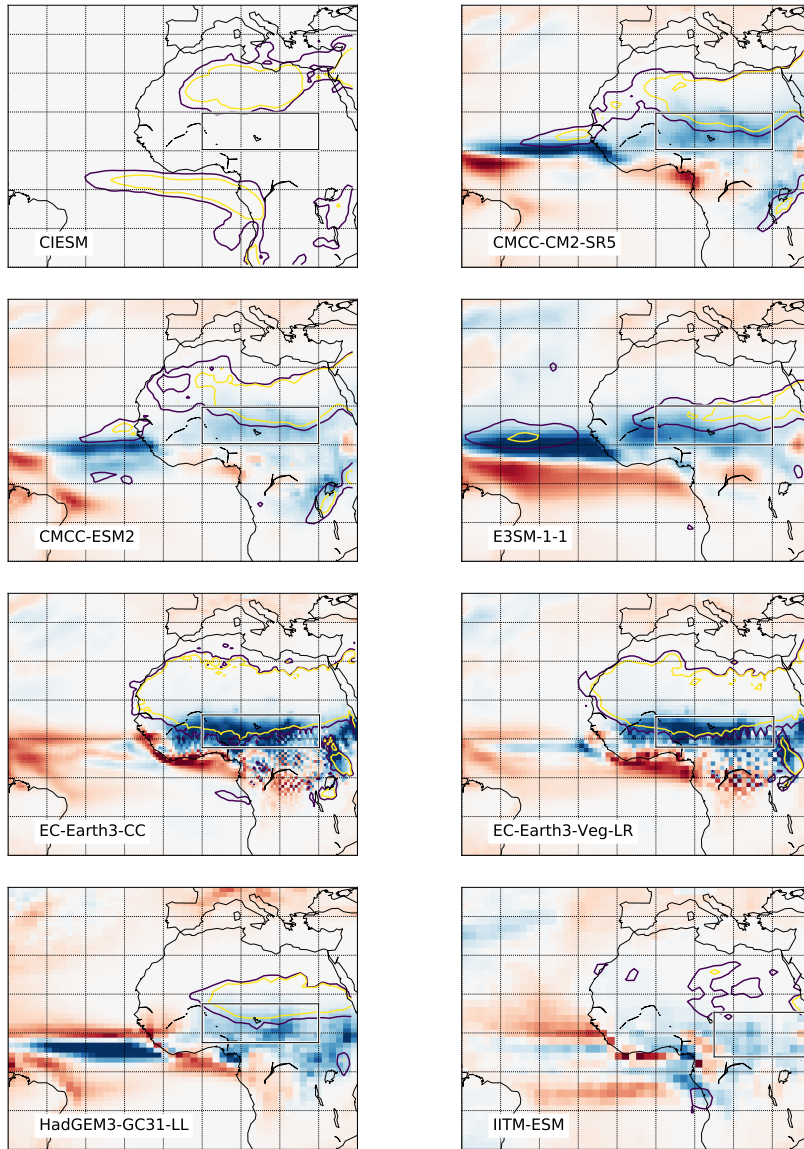


Figure S3. continued.

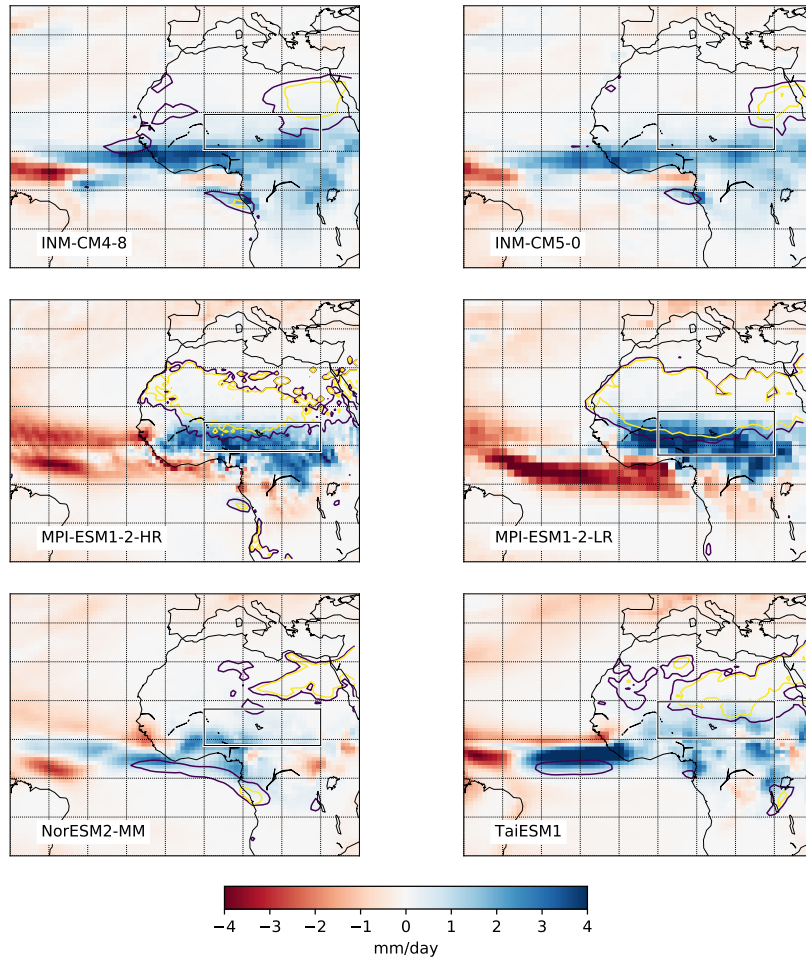


Figure S3. continued.

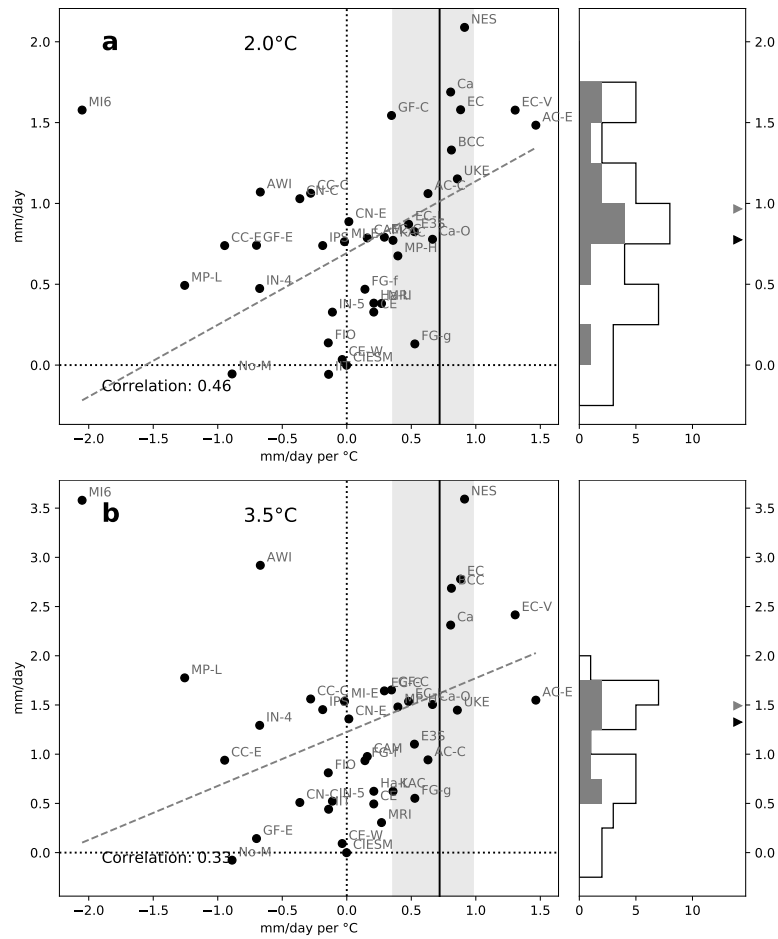


Figure S4. As Fig. 3 in the main paper but with simulated precipitation averaged for each model separately over a rectangular region of particularly strong precipitation change, outlined in Figure S3.